Optical constants of as-deposited and treated alkali halides, and their VUV quantum efficiency

Juan I. Larruquert[1], José A. Méndez, José A. Aznárez

Instituto de Física Aplicada, CSIC
28006 Madrid (Spain)

Anton S. Tremsin, Oswald H.W. Siegmund

Space Sciences Laboratory
UC Berkeley
Berkeley, CA 94720

ABSTRACT

The optical constants of thin films of CsI, KI, and KBr in the spectral range of 53.6-174.4 nm were obtained from the measurements of reflectivity as a function of the incidence angle. The effect of film heating to 420 K and exposure to UV radiation on the optical constants of the three materials was also investigated. The quantum efficiencies (QEs) of the planar photocathodes made with the three alkali halides, as well as the changes in these QEs after the photocathode treatment similar to that applied to the thin films was measured. KBr was found to be the most stable to heating and irradiation. KI appeared to be close to temperature-stable, while UV exposure affected its optical constants. CsI optical constants were changed after 420-K heating, as well as after UV exposure. The changes in the optical constants were related to the QE changes and the correlation between these variations was determined.

Keywords: Photocathodes, Quantum Efficiency, Alkali Halides, CsI, KI, KBr

1. INTRODUCTION

The photocathodes made with alkali halides have attracted considerable interest in recent years, as they provide an efficient means for UV photon conversion over a wide spectral range of the extreme UV (EUV) and far UV (FUV) radiation. Among these materials, CsI, KI and KBr exhibit relatively high quantum efficiency (QE) values, and therefore they are extensively used for EUV-FUV detection.

The stability of alkali halide photocathodes is important for practical applications. The effect of photocathode heating and exposure to UV radiation on the QE has been investigated by several groups, mainly for CsI photocathodes[1-7]. Changes in the QE may be attributed to changes in the optical properties of the photocathode film and/or changes in the electron transport properties and electron escape probability. In this paper we investigate the optical costants of thin films of the three alkali halides and of heating them and exposing them to UV radiation. We also directly measured the changes in QEs of the planar photocathodes made with the three materials, and calculated their QE variations using the measured optical constants and assuming that the photoelectron transport properties remain unchanged after the treatment. The measured and calculated values of QE variations were then compared.

2. EUV-FUV OPTICAL CONSTANTS OF CSI, KI, AND KBR

---

[1] Correspondence: Email: larruquert@io.csic.es; Telephone: 34 91 561 6800; Fax: 34 91 564 5557

In this section we describe the preparation of thin films of CsI, KI, and KBr, the measurements of EUV-FUV reflectivity, the treatment given to the samples, and calculation of optical constants (this work was performed at the Metal Optics Laboratory (MOL), Instituto de Fisica Aplicada, CSIC, Madrid).

2.1. Experimental techniques

The thin film deposition, reflectivity measurements and sample treatment were performed in the MOL EUV-FUV reflectometer described elsewhere [8, 9]. This device works under ultra-high vacuum (UHV) conditions and covers reflectivity measurements in the spectral range of 50-200 nm, for incidence angles varying from near-normal to near-grazing. The reflectometer is equipped for in situ UHV thin film deposition. Fig.1 shows a schematic view of the equipment. The system incorporates the sample transfer chamber, the deposition chamber and the reflectometer chamber. The chambers are connected through gate valves and long sample manipulators. The reflectometer and deposition chambers were each pumped with an ion pump and a titanium sublimation pump. The sample transfer chamber was used for the sample transfer without breaking vacuum. This chamber was pumped with a turbomolecular pumping system, and was provided with a Penning gauge and a MgF_2 window for UV exposure. The reflectometer chamber was baked out to 470 K. For the present work the deposition chamber was not baked out.
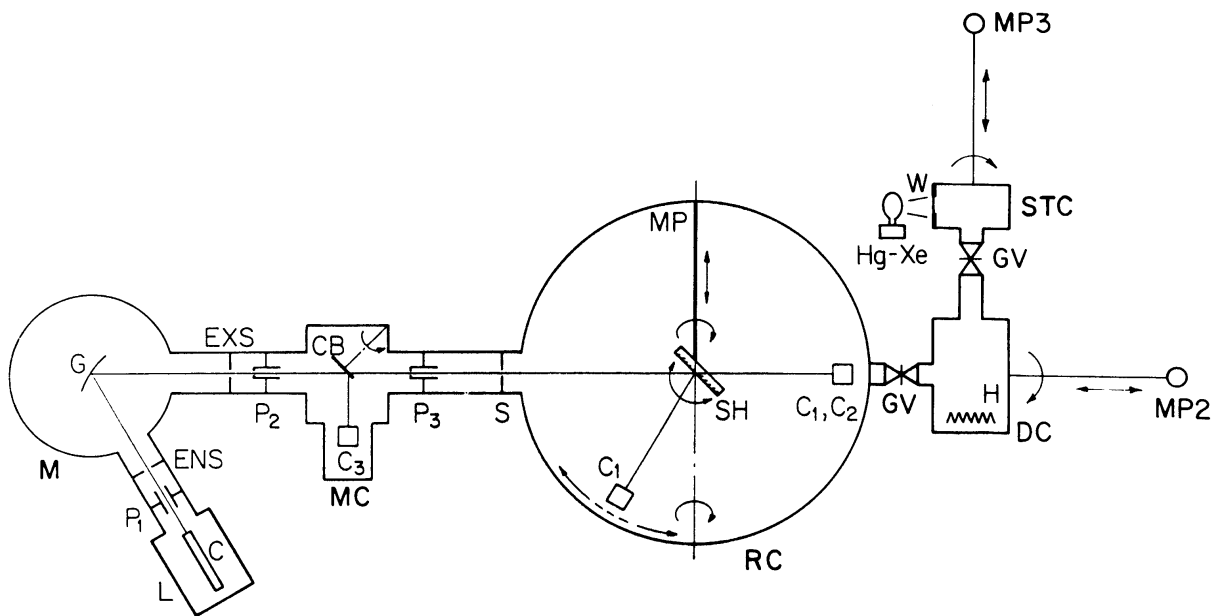

Fig. 1. Schematic view of the experimental equipment: C: capillary; L: lamp; M: monochromator; G: diffraction grating; ENS: entrance slit; EXS: exit slit; MC: modulation chamber; CB: chopper blade; S: aperture stop; RC: reflectometer chamber; C_1, C_2 and C_3: channel electron multipliers; MP, MP2, MP3: sample manipulators; SH: sample holder; P_1, P_2 and P_3: small conductance pipes; DC: deposition chamber; STC: sample transfer chamber; GV: gate valve; H: sample heater; W: MgF_2 window; Hg-Xe: Hg-Xe lamp for UV exposure.

The deposition chamber was provided with a quartz crystal thickness monitor, an ion gauge, a residual gas analyzer, and a radiant sample heater. An alkali halide was sublimated from Ta boats combined with a K thermocouple to control the operation temperature. 99.999% purity powder CsI, KI and KBr were used. The film thickness was calibrated using Tolanski interferometry. Prior to deposition, the boats and powders were thoroughly outgassed up to temperatures close to that required for sublimation. The deposition process was controlled with a shutter and performed at a typical rate of about 1.2 nm/s. A thickness of 400 nm was selected as a value close to those used in the preparation of photocathodes, which was large enough to ensure that the substrate influence would be negligible. Along with that, some films as thin as 50 nm were also deposited and studied. In the case of KBr, a thickness of 100 nm was found to maximize EUV reflectivity.
The resistive sample heater consisted of a toroidal resistance coil positioned 4.5 cm below the sample. The temperature of the samples was controlled using a K thermocouple placed in contact with their surface.

Typical pressures at different experiment stages comprised 3×10^{-8} Pa for the base pressure in the reflectometer chamber (when isolated from the lamp-monochromator), 2×10^{-7} Pa in the non-baked deposition chamber, about 5×10^{-6} Pa during alkali halide deposition, 10^{-6} Pa during sample heating, and 10^{-5} Pa during UV exposure. The total pressure in the reflectometer during reflectivity measurements was 3×10^{-7} Pa, while the residual atmosphere in it mainly consisted of the non-oxidizing gas mixture flowing in the discharge lamp, which reached the UHV reflectometer chamber through a differential pumping arrangement. The gas mixture was composed of 93% He, 3% Ne, 3% Ar, and 1% N_2. The reflectivity measurements were performed at room temperature.

The exposure of samples to UV radiation was performed in the sample transfer chamber using an ORIEL (model 68752), 200-W, Hg-Xe lamp placed in front of the MgF_2 window. The lamp was used with no filter and was calibrated to provide the radiation flux at the sample of 4.3 mW/cm^2 at the 253.7 nm Hg line.

The sample treatment and reflectivity measurements were performed as follows. A thin film of an alkali halide was deposited onto a 50.8-mm x 50.8-mm x 3-mm floated glass substrate. The subsequent procedure consisted of several stages. First, immediately after deposition, the sample was transferred to the reflectometer chamber, and its reflectivity was measured in the spectral range of 53.6-174.4 nm, for 9 incidence angles between 5° and 80°. At the second stage, the sample was transferred back to the deposition chamber and heated to 370±25 K for 5 hours. Following that, it was placed in the reflectometer chamber, and its reflectivity after heat treatment was measured. At the third stage, the sample was transferred to the deposition chamber again and heated to 420±25 K for 2 hours. Then it was placed in the reflectometer chamber for the next measurement of its reflectivity. Sample was allowed to cool down before measuring reflectivity. At the final stage, the sample was transferred to the sample transfer chamber, where it was exposed to UV radiation from Hg-Xe lamp for 8 hours. After this last treatment, the sample was placed back to the reflectometer chamber, and its reflectivity after the UV exposure was measured. All these processes and transfers were carried out without breaking vacuum.

2.2. The optical constants of alkali halides

The measurements of reflectivity as a function of the incidence angle were performed in the horizontal plane of incidence, for 9 angles varying from 5º to 80º. The radiation from the monochromator was partially polarized. The polarization degree, along with the optical constants of the glass substrates used, had been determined prior to the reflectivity measurements. The reflectivity of the glass substrates was measured in two perpendicular planes of incidence: horizontal and vertical. Once the polarization degree was determined for every wavelength, it was assumed to be a fixed parameter of our reflectometer. The optical constants of the glass substrates and the polarization degree of radiation were used in the calculation of the optical constants of alkali halides. This calculation took into account the influence of the interface between the thin film and the substrate, while surface roughness was neglected. The optical constants n and k were obtained as parameters minimizing the squared difference between the measured and calculated values of reflectivity, added over all incidence angles. More details on optical constant calculation were given elsewhere [10].

2.2.1. CsI films

Fig.2 shows the optical constants for a 400-nm thick, CsI film, and also for the same sample, after it was heated to 370 K for 5 hours, then heated to 420 K for 2 hours, and finally exposed to UV radiation for 8 hours. We can see that heating the sample to 370 K had almost no effect on the CsI optical constants. The further temperature increase to 420 K resulted in a decrease of the imaginary part of the refractive index k in the whole spectral range investigated, whereas the real part, n, did not change significantly. Exposing the sample to UV radiation resulted in a further decrease of k for wavelengths of 120.0 nm and above, and a small increase in n for wavelengths over 113.5 nm. The sharp peak, exhibited by k at 93.1 nm for the as-deposited film, remained unchanged after heating to 370 K, but almost disappeared after the further heating to 420 K. The peak of n at 96.4 nm also kept constant after heating the sample to 370 K, but lowered considerably after the subsequent heating to 420 K.
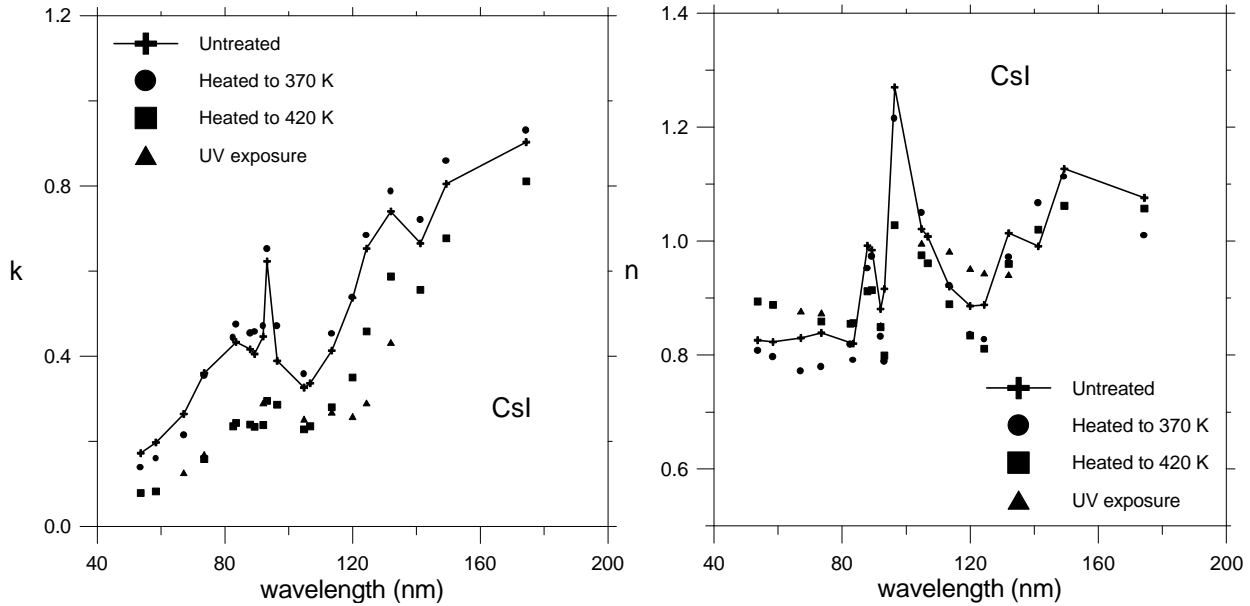
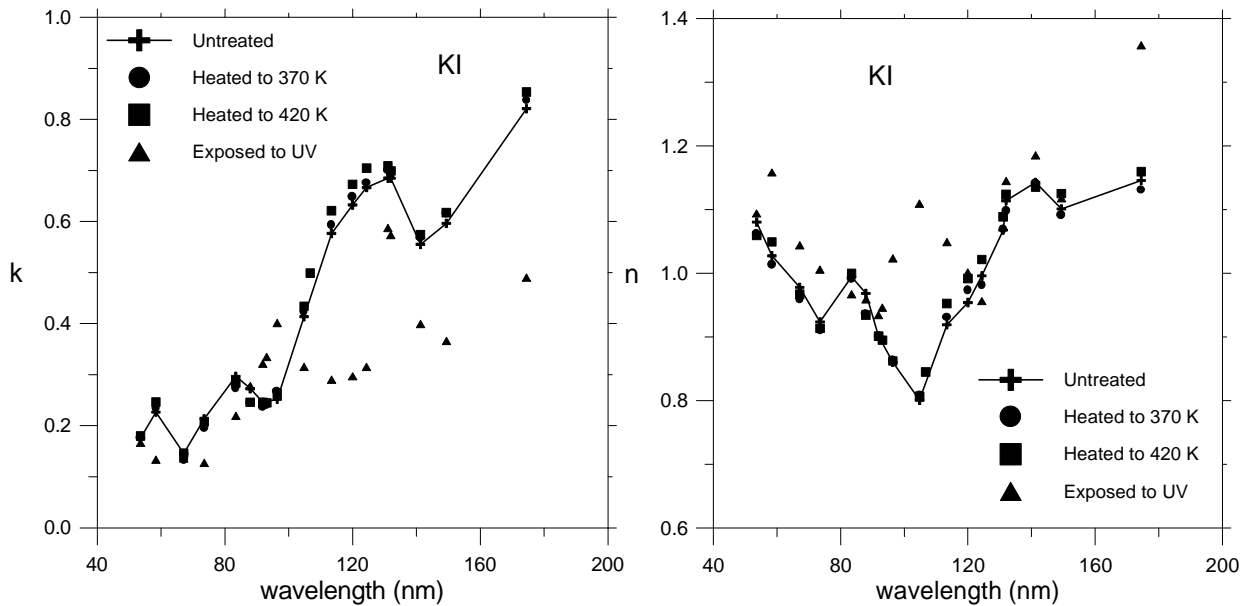Fig. 2. Optical constants of a 400-nm thick, CsI film.

Fig. 3. Optical constants of a 400-nm thick, KI film.

2.2.2. KI films

Fig.3 shows the optical constants for a 400-nm thick, KI film, and also for the same sample, after it was heated to 370 K for 5 hours, then heated to 420 K for 2 hours, and finally exposed to UV radiation for 8 hours. Heating KI films to 420 K produced no significant change in the optical constants in the whole spectral range. However, the exposure to UV radiation had a pronounced effect on the optical constants. The extinction coefficient k of the sample exposed to UV exhibited completely

different values for wavelengths of 92.0 nm and above, while its maximum at 132.0 nm disappeared. The refractive index n was higher than that for the as-deposited and the heated sample in the whole spectral range, with a maximum located at 92.0 nm, just where n for both the as-deposited and the heated sample had a minimum.

2.2.3. KBr films

Fig.4 shows the optical constants for a 100-nm thick, KBr film, and also for the same sample, after it was heated to 420 K for 2 hours, and finally exposed to UV radiation for 8 hours. In the case of KBr, the reflectivity of 50-100-nm thick films resulted in a higher normal EUV-FUV reflectivity than that for 400-nm thick films (this difference might be attributed to a smoother and/or more compact structure of 50-100-nm thick films). For that reason, we decided to investigate the optical constants of a 100-nm thick film. The optical constants of KBr did not change significantly after heating the sample to 420 K or after UV exposure. The only considerable change was in the peak of n that shifted from 113.5 nm for the as-deposited and the heated film to 124.4 nm for the UV-irradiated film.

To summarize, no significant change was observed in the optical constants of the 3 alkali halides after their heating up to 370 K. Heating up to 420 K still had almost no effect on KI and KBr, although it decreased significantly the extinction coefficient of CsI. Finally, UV exposure to a 200-W Hg-Xe lamp for 8 hours had only a slight effect on the refractive index of KBr around 120 nm, whereas it lowered further the extinction coefficient of CsI for wavelengths over 113.4 nm, and somewhat lowered the extinction coefficient of KBr, with an important change in the refractive index at 92.0 nm.
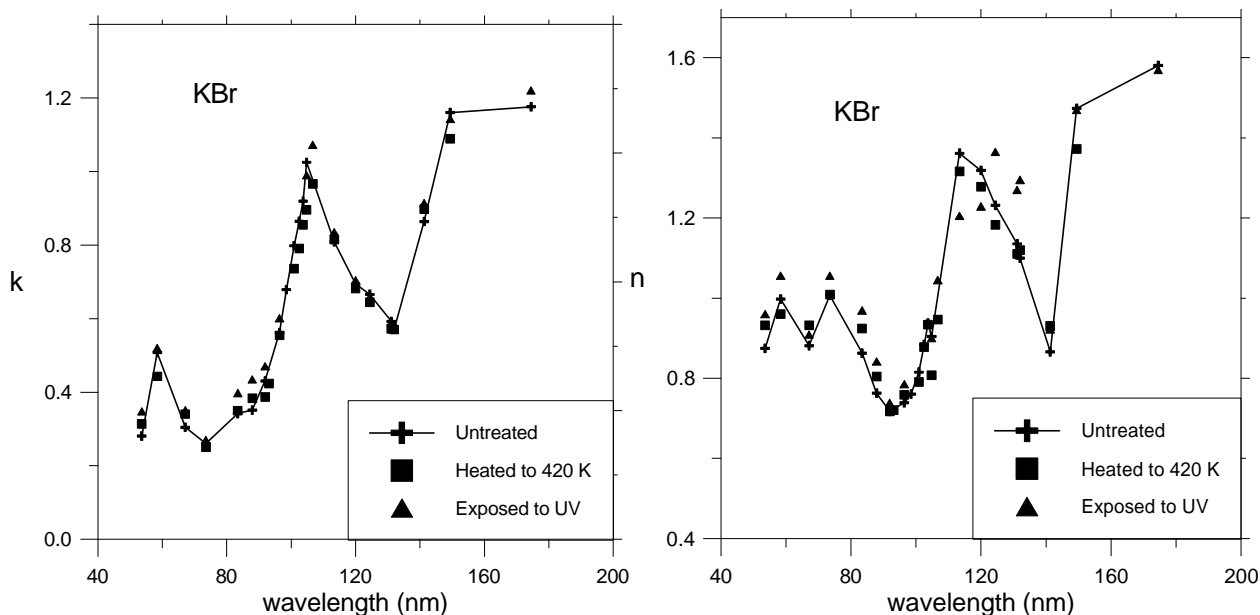

Fig. 4. Optical constants of a 100-nm thick, KBr film.

3. OPTICAL CONSTANTS AND PHOTOCATHODE QUANTUM EFFICIENCY

In this section we discuss the photocathode quantum efficiency (QE) variation with heat treatment and UV exposure. First we calculate the QE variation from the measured optical constants with the help of the model suggested by Fraser[11], assuming that only the optical properties of the evaporated layers change with the treatment, while other model parameters remain

constant. Then we compare the calculated results with the experimentally measured QE variation of CsI, KI and KBr photocathodes, thus verifying the significance of the changes in the electron transport properties and electron escape probability after the heating and UV exposure.

3.1. Photocathode preparation and QE measurements

All the quantum efficiency measurements described below were carried out for planar reflective photocathode samples at normal incidence angle. CsI, KI and KBr layers (~800 nm thick) were evaporated on polished stainless steel substrates (4x4 cm^2) at a rate of ≤2.0 nm/s and at pressures ~2.6x10^{-4} Pa. After the deposition the chamber was purged with dry nitrogen and then all samples were briefly exposed to the air during the transfer from the deposition station to the vacuum chamber. All QE measurements, heat treatment and UV exposure were performed at pressures ~10^{-5} Pa and at room temperatures. The samples were mounted on the front face of a custom-made electrometer, which allowed us to measure the photocurrent with an accuracy of about 0.5 femtoamps. A positively-biased grid was positioned 3 mm in front of the photocathodes to provide photoelectron collection. The quantum efficiency of the photocathodes was measured with monochromatic radiation provided by a gas discharge hollow cathode source in combination with a 1 m grazing incidence monochromator. Absolute QEs were derived from the flux measurement comparisons with a reference standard - a NIST-calibrated photodiode. The spectral response of the as-deposited photocathodes was measured several hours after the deposition and then re-measured after the heat treatment and UV exposure. The study of UV radiation during aging was provided by a mercury vapor pen-ray lamp, installed in the chamber at a distance of ~0.5 m from the samples. A NIST-calibrated far ultraviolet windowed photodiode was used to calibrate the incident photon flux from the lamp, and at the plane of the samples it was measured to be 1.15x10^{10} and 4x10^8 photons/mm^2/sec for 253.7 and 184.0 nm wavelengths, respectively. The thermally-treated samples were heated from the rear side with a resistive heater to temperatures of about 360 K for several hours and then allowed to cool down to room temperature over a period of several hours.

3.2. QE calculations

The model we used in our QE calculations was suggested by Fraser[11], which for normal incidence yields the following formula:

$$QE = [1 - R(normal)] f P_s(0) E_x \boldsymbol{e}^{-1} (1 + \boldsymbol{b})^{-1} \left[1 - \exp\left(-(1 + \boldsymbol{b}^{-1}) \frac{T}{L_s} \right) \right] \qquad (1)$$

$$\boldsymbol{b} = (\boldsymbol{m} \cdot L_s)^{-1},$$

where R(normal) is the specular reflection coefficient at a normal angle, E_x is the photon energy, $\boldsymbol{e}$ is the energy required to produce one photoelectron, f is the fraction of the photon energy available for creation of photoelectrons, $P_s(0)$ is the electron escape probability on the surface, T is the photocathode thickness, $\boldsymbol{m}$ is the linear absorption coefficient and L_s is the electron escape length. R(normal) and $\boldsymbol{m}$ can be calculated from the optical constants as follows:

$$R(normal) = \frac{(n-1)^2 + k^2}{(n+1)^2 + k^2} , \qquad (2)$$

$$\boldsymbol{m} = 4\boldsymbol{p}k / \boldsymbol{l} ,$$

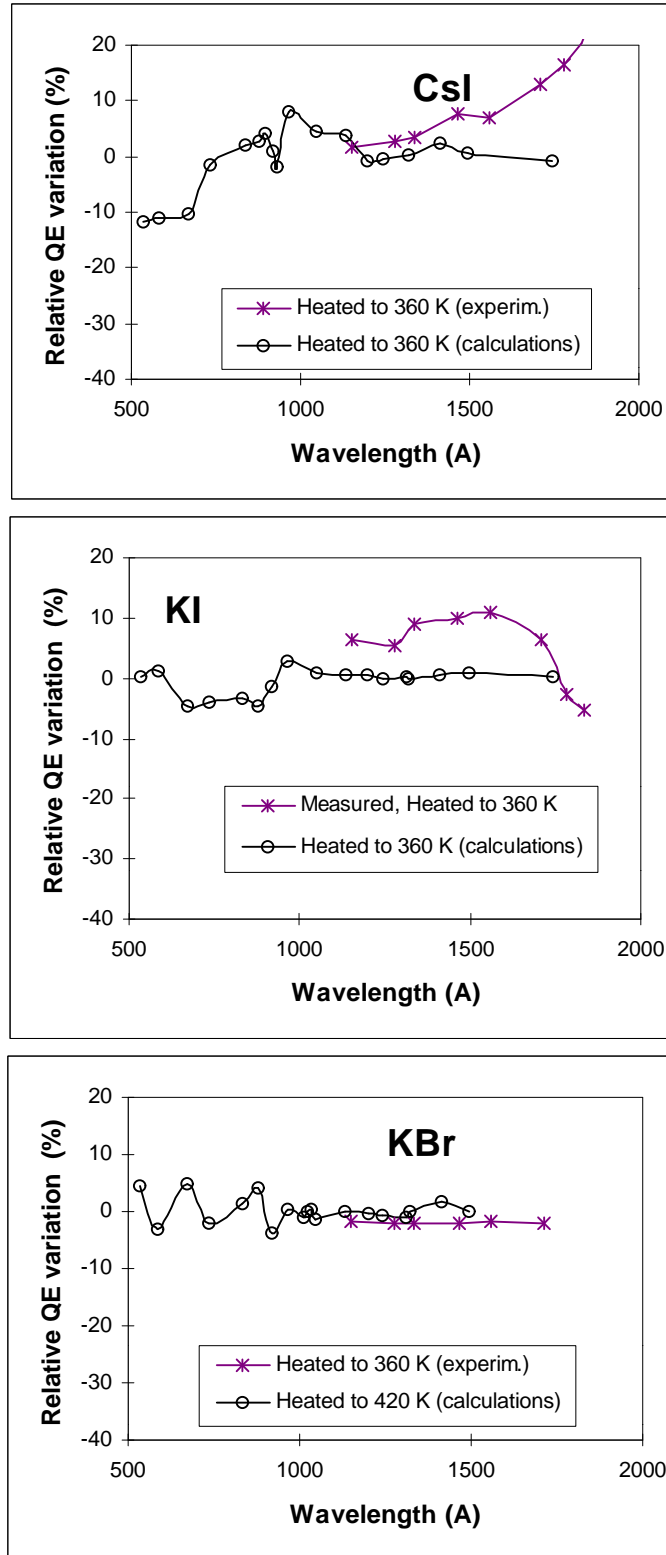where n and k are the optical constants of the photocathode material.

Fig.5. QE as a function of wavelength measured after heating the samples (QE^{heated}) normalized to the as-deposited QE value (QE^0). The experimentally measured QE changes were obtained with planar reflective photocathode samples. The calculated QE's were obtained from formula (3) with the optical constants measured for heated films (Section 2.2, Figs.2-4).
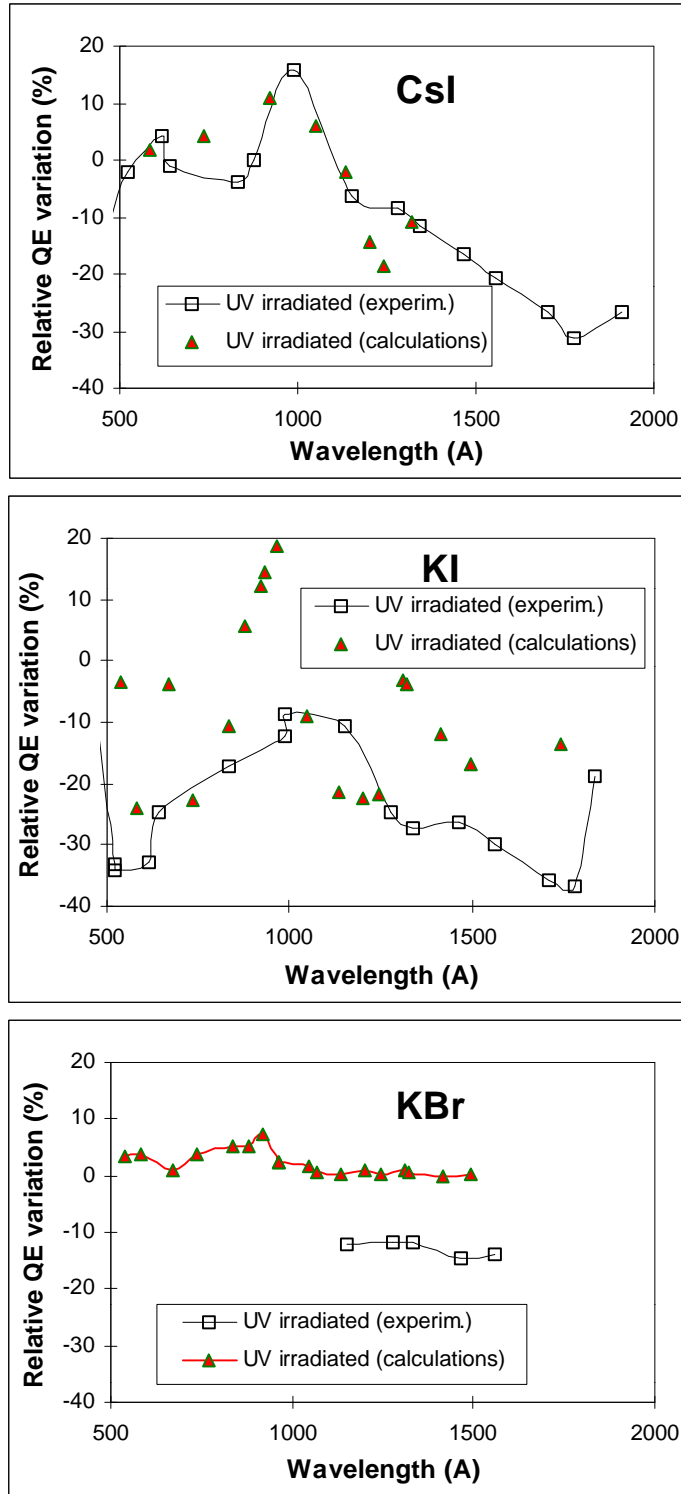
Fig.6. QE as a function of wavelength measured with UV-irradiated photocathodes (QE^{UV}) normalized to the QE values measured before irradiation (QE^{heated}). The experimentally measured QE changes were obtained with planar reflective photocathode samples, which were irradiated by UV flux of 1.15×10^{10} photons mm^{-2} sec^{-1} at 253.7 nm at the plane of the samples with total dose of 8×10^{14} photons. A mercury vapor pen-ray lamp placed in the vacuum chamber was used for the illumination. The calculated QE's were obtained from formula (3) with the optical constants measured for UV-irradiated films (Section 2.2, Figs.2-4).

To calculate QE variation after UV exposure and heat treatment, in addition to the data on optical properties, we have to know the variation of other parameters, namely e, f, $P_s(0)$ and L_s. The changes in electron escape length L_s should correspond to the transformation of the photocathode material in the bulk, while the value of $P_s(0)$ is determined by the surface properties. We cannot compare the results of our calculations with the experimentally obtained QE variation, since we do not possess information about the deviation of the photoelectron excitation, transport and escape parameters. By assuming they remain constant and comparing the calculated results with the measured data, we can determine whether the photoelectron parameters are transformed by UV exposure and heat treatment. With this assumption, the relative QE variation can be estimated from the following equation:

$$\frac{QE}{QE^0} = \frac{1-R}{1-R^0} \frac{(1+b^0)}{(1+b)} \left[1 - \exp\left(-\left(1+b^{-1}\right)\frac{T}{L_s}\right)\right] \cdot \left[1 - \exp\left(-\left(1+\frac{1}{b^0}\right)\frac{T}{L_s}\right)\right]^{-1} \qquad (3)$$

Fig.5 shows the ratio between the quantum efficiency values calculated with the optical constants (n,k) measured before and after heat treatment, while Fig.6 shows the ratio between the QE calculated with (n,k) measured after UV radiation and after heat treatment of the sample. The values of parameter L_s were taken from Refs.[12-16]. The experimentally measured (Section 3.1) QE variation data is also presented in Figs 5, 6.

4. CONCLUSIONS

The results of the optical constant measurements showed that, among the three photocathode materials studied, KBr is the most stable to thermal treatment and UV irradiation. Its optical constants were barely affected after the treatment, while those for KI thin film exhibited the largest change after being exposed to UV radiation. The optical constants of CsI film changed after both heating and UV irradiation. Our direct measurements of photocathode quantum efficiency variation after a similar treatment were compared to QE changes calculated from the optical constants under an assumption that the photoelectron transport properties remain unchanged. The distinctions revealed by this comparison confirm the significance of accounting for variation of such parameters as the electron escape probability and escape length with heating and UV exposure. We can conclude that changes in the optical properties of CsI, KI and KBr photocathodes cannot solely explain the observed QE changes, but the electron transport properties should also be considered. CsI QE decrease with UV irradiation is the only case which can probably be attributed to changes in the optical constants (n,k). This is likely to be due to the formation of color centers in CsI, changing both the UV absorption coefficient and the photoelectron escape length. A further study of the influence of heat treatment and UV irradiation on photocathode performance (regarding its structure and photoelectron transport properties) is required for a better understanding of photocathode response and stability.

5. ACKNOWLEDGMENTS

6.REFERENCES

1. D.F. Anderson, S. Kwan, V. Peskow, and B. Hoeneisen, "Properties of CsI and CsI-TMAE photocathodes", Nucl. Instr. and Meth. **A 323**, 626 (1992).

2. H. Brauning, A. Breskin, R. Chechik, P. Mine, and D. Vartsky, "Investigation of CsI and CSI-TMAE VUV-photocathodes in vacuum and gas media", Nucl. Instr. and Meth. **A 327**, 369 (1993).

3. J. Almeida, A. Braem, A. Breskin, A. Buzulutskov et al. "Microanalysis surface studies and photoemission properties of CsI photocathodes", Nucl. Instr. and Meth. **A 367**, 337 (1995).

4. A. Buzulutskov, A. Breskin, and R. Chechik, "Heat enhancement of the photoyield from CsI, NaI and CuI photocathodes", Nucl. Instr. and Meth. **A 366**, 410 (1995).

5. G.W. Fraser, S.E. Pearce, J.F. Pearson, V.N. Schemelev, A.P Pavlov, and A.S. Shulakov, "Thermally annealed soft X-ray photocathodes", Nucl. Instr. and Meth. **A 381**, 453 (1996).

6. J. Vavra, A. Breskin, A. Buzulutskov, R. Chechik, and E. Shefer, "Study of CsI photocathodes: Volume resistivity and ageing", Nucl. Instr. and Meth. **A 387**, 154 (1997).

7. A.S. Tremsin, O.H.W. Siegmund, "Heat enhancement of radiation resistivity of evaporated CsI, KI and KBr photocathodes", Proc. 2nd International Conference "New Developments in Photodetection", Beaune, France, June 21-25, 1999 (to be published in Nuclear Instruments and Methods in Physics Research (section A).

8. J.I. Larruquert, J.A. Méndez, and J.A. Aznárez, "Far-UV reflectance of UHV-prepared Al films and its degradation after exposure to O_2", Appl. Opt. **33**, 3518-22 (1994).

9. J.A. Aznárez, J.I. Larruquert, and J.A. Méndez, "Far-ultraviolet absolute reflectometer for optical constant determination of ultrahigh vacuum prepared thin films", Rev. Sci. Instrum. **67**, 497-502 (1996).

10. J.I. Larruquert, J.A. Méndez, and J.A. Aznárez, "Far-ultraviolet reflectance measurements and optical constants of unoxidized aluminum films", Appl. Opt. **34**, 4892-4899 (1995).

11. G.W. Fraser, "The characterisation of soft X-ray photocathodes in the wavelength band 1-300 Å", Nucl. Instr. and Meth. **206,** 251-263 (1983).

12. S.R. Jelinsky, O.H.W. Siegmund, and J.A. Mir, "Progress in soft x-ray and UV photocathodes", *Proc. SPIE* **2808,** 617-625 (1996).

13. T. Boutboul, A. Akkerman, A. Breskin, and R. Chechik, "Escape length of ultraviolet induced photoelectrons in alkali iodide and CsBr evaporated films: Measurements and modeling", J. Appl. Phys. **84**, 2890-2896 (1998).

14. A. Akkerman, T. Boutboul, A. Breskin, R. Chechik, and A. Gibrekhterman, "Low-energy-electron transport in alkali-halides", J. Appl. Phys. **76,** 4656-4662 (1994).

15. O.H.W. Siegmund, E. Everman, J.V. Vallerga, J. Sokolowski, and M. Lampton, "Ultraviolet quantum detection efficiency of potassium bromide as an opaque photocathode applied to microchannel plates", Appl. Opt. **26,** 3607-3614 (1987).

16. A. S. Tremsin, O. H. W. Siegmund,, "Incidence angle dependence and stability of quantum efficiency of alkali halide photocathodes", within this volume (*Proc. SPIE* **3765**, 1999).